# Computer-generated complex filter for an all-optical and a digital-optical hybrid correlator

**Philip Birch**
**Rupert Young,** MEMBER SPIE
**Frédéric Claret-Tournier**
**David Budgett**
**Christopher Chatwin,** MEMBER SPIE
University of Sussex
School of Engineering and Information
    Technology
Brighton, East Sussex BN1 9QT, UK
E-mail: p.m.birch@sussex.ac.uk

**Abstract.** We present results of a correlation filter utilizing a computer-generated hologram using an analog ferroelectric liquid-crystal spatial light modulator (SLM). The SLM amplitude-modulates light and can induce a 0-$\pi$ phase shift, which is equivalent to modulating along the real axis. Two pixels are combined into a macropixel using a phase-detour technique enabling full complex modulation. The method is used as the filter for a conventional optical correlator and in a digital-optical hybrid correlator. © *2002 Society of Photo-Optical Instrumentation Engineers.*
[DOI: 10.1117/1.1425785]

## 1 Introduction

Correlators enable high-speed image and character recognition. One of the usual configurations for such a device is based on the Vander Lugt[1] design. Images are captured by a CCD camera and displayed on an intensity-modulating spatial light modulator (SLM). This is then optically Fourier-transformed onto the filter-plane SLM. In order to test many templates, the filter SLM must work at a much higher speed than the input SLM. Several kilohertz is often required if the input camera SLM is updated at normal video rate. A common technique to achieve this is to use a conventional bistable smectic C* ferroelectric liquid crystal (FLC) SLM. However, this type only produces a binary-phase-only filter (BPOF), which is vulnerable to input noise, object rotation, and scaling. It would therefore be more desirable to produce a filter that not only can be updated at high speed but also is capable of full complex modulation. In this paper we discuss the construction of such a filter and demonstrate its use in a correlator system.

In modern 4-f optical correlators, the two Fourier transformations and the mixing of the input signal with the reference signal are performed optically, and the data handling and control are usually managed by a computer. The filter spectrum is generally phase-modulated by an electrically addressed SLM in the frequency domain. The BPOF FLC SLM controlled by digital electronics has proved an effective solution.[2] This method has been preferred by many system developers recently, several well-engineered prototype systems having been developed largely, but not exclusively, for missile terminal guidance applications.[3] Extensive research has shown that binarization of the Fourier-plane phase generates a good correlation response, the correlation peak being remarkably resistant to such gross frequency-plane quantization. However, binarization of the input scene is less effective, particularly for unconstrained scenes in which the lighting levels are unknown and variable. Thus, an SLM capable of binary amplitude modulation can only be used as the input modulator to an optical correlator if the scene acquired from the input camera has

been digitally preprocessed in a sophisticated manner. Even then, input-plane binarization still restricts the effectiveness of the correlation-based pattern recognition.

In general, the input scene does not need to be updated at the kilohertz frame rates achievable with binary-effect SLMs; often the 25- to 30-Hz frame update rate associated with standard video sources is adequate. Thus, SLMs capable of generating a gray-level response may be used as the input device to the optical correlator, the input scene being introduced to the correlator with minimal preprocessing. However, there are many problems associated with doing this.[4] A particularly important development for the optical processing community in recent years has been the availability of devices based on analog ferroelectric liquid crystals (AFLCs).[5] With appropriate configuration of the polarizer, such devices can be made to generate a bipolar analog response (along the real axis of the complex plane) and so are useful both in the input and in the frequency plane of a coherent optical correlator.[6] The ability to use identical devices with exact pixel matching in both spatial and frequency planes will greatly facilitate the design of all optical correlators.

### 1.1 Problems in Designing a Compact Optical Correlator

The specific characteristics of the SLM devices employed are all important in the design problems faced in realizing a compact and robust optical correlator. The main problem is to accurately match the Fourier transform of the scene displayed on the input SLM to the spectrum displayed on the frequency-plane SLM, together with the maintenance of this match in the face of (possibly severe) environmental disruption. Thus, all optical correlators that meet demanding military and industrial requirements present far from trivial electro-optic and optomechanical design problems, which have only been partially solved in the current state of the art. The problems inherent in the design of an all-optical correlator can be summarized as follows:
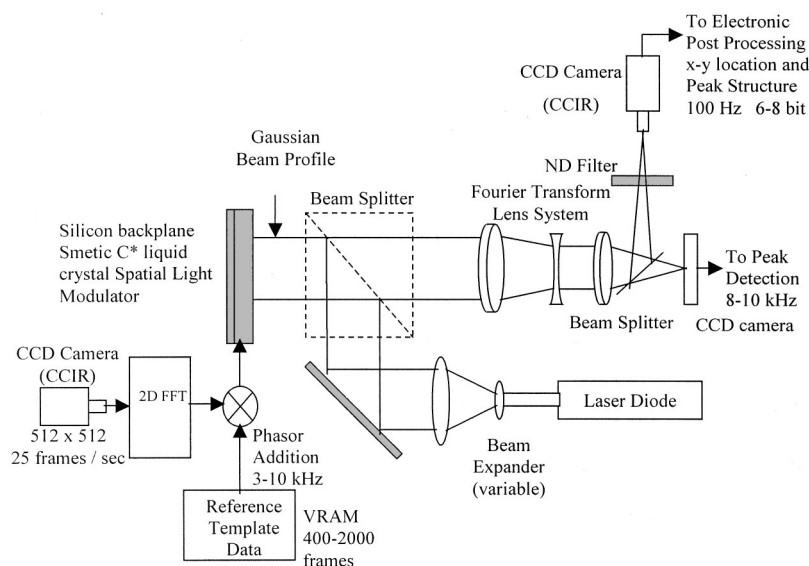
Fig. 1 Schematic layout of digital-optical hybrid correlator.

- The input SLM is required to produce a large-dynamic-range analog image with high optical quality and a high data transfer rate.

- The mechanical stability of the optical system must be very high. The pixel size of a typical current device is $\approx 40 \ \mu$m, and this number is constantly being reduced as pixels become smaller. For optimum performance the optical spectrum must be kept aligned to less then one pixel displacement. This is a problem in the commercial development of correlator systems when the end user may not have the technical knowledge to align the system.

- The small pixel size is also demanding on the optical design of the Fourier-transform lens systems. The lens design requirements are complex if a compact correlator arrangement is to be realized. This is further complicated by the need to illuminate the input SLM uniformly. This turns out to be a nontrivial problem. A laser usually gives a Gaussian beam profile; either it needs to be sampled, which is very wasteful of beam power, or diffractive optical elements are required, which introducing a random phase into the input and also require highly stable laser sources.

### 1.2 Hybrid Digital-Optical Design

The hybridization with digital electronics can be taken a stage further. Digital signal processing can be used to overcome several of the problems listed above by replacing the first Fourier transform of a conventional correlator system with its electronic equivalent. This arrangement is shown schematically in Fig. 1. To overcome problems with the input SLM, the scene is captured with a CCD camera, and its fast Fourier transform (FFT) is evaluated electronically. The complex data are then mixed with reference filters and placed on a SLM. This SLM is then optically Fourier-transformed onto a high-speed camera that records the results. This method has several advantages over conventional correlators: The input SLM is avoided, so the spectrum of the input signal is no longer degraded by im-

perfections of the SLM. The power levels required of the laser are less, and there is no longer a need for uniform illumination. The optical design of the system is greatly simplified, since only one Fourier transform lens is required. This in turn increases the compactness of the system and greatly increases its mechanical robustness.

The computer in this system has taken over two functions previously performed optically: the Fourier transformation of the input signal, and the mixing of the complex spectrum with the filter functions. The FFT is computationally more intensive than the mixing function. However, for an image recognition task only video rates (25 Hz) are usually required for the input, while the mixing is limited to either the frame speed of the SLM or the frame speed of the camera. The basic principle of the system is to grab the input signal, FFT it at video rate, and then mix the resulting data with predesigned filter functions and place the results on the SLM. The SLM is uploaded faster than the FFTs are evaluated, so that a large number of filters can be tested for each input FFT. The concept of combining a digital and an optical Fourier transformation into a hybrid correlator system was first reported a number of years ago by the authors,[7] but a high-speed hardware realization has only recently been possible. The design and construction of such a correlator is discussed in Ref. 4 and is summarized as follows.

The system uses eight SHARC floating-point DSP processors that are capable of producing a $512 \times 512$ FFT at a rate of 25 frames/s. The input-scene camera is a digital DALSA camera, and the data are fed into the SHARC processors via a field-programmable gate array (FPGA) chip. A further two SHARCs and one FPGA are used to perform the multiplication between the input spectra and the template filters and write the resulting data to the SLM controller. A high-frame-rate DALSA camera ($128 \times 128$ pixels and $\approx 800$ Hz) is synchronized with the SLM and records the correlation image. Another FPGA and SHARC processor interface with this camera to perform the peak detection.

The system was originally designed to use a BPOF. A fully complex filter would perform closer to the ideal filter, and this paper assesses the design of such a filter. The filter is demonstrated experimentally in a conventional 4-f correlator and in the hybrid mode of operation.

Several authors have demonstrated full complex modulation before. One method of achieving this is by cascading two SLMs together[8]—either one amplitude-modulating SLM and another phase-modulating SLM, or two different twisted nematic SLMs. Two SLMs proved a simple solution, but unfortunately increased the bulk of the system and its cost. Single-SLM methods have involved blurring together pixels of deformable mirrors[9,10] and using four pixels of the SLM for each datum.[11] Several authors have used the phase-detour technique.

However, not all of these methods can be easily realized on a pixelated SLM. Lee[12] proposed a four-pixel phase-detour technique where the complex datum is split into its positive real, positive imaginary, negative real, and negative imaginary components. These components are then placed on adjacent pixels. The complex datum point will then be realized off axis, where a $\pi/2$ phase lag exists between pixels. The four pixels required were later reduced to three pixels[13] by sampling the 0-, 120-, and 240-deg components. Unfortunately, SLM design is limited in resolution, and so ideally the least possible number of pixels should be used to represent a complex datum point. There is also a large dc associated with the Lee technique. The method used in this paper reduces the number of pixels required to two, effectively doubling the resolution, and removes the dc term as explained below.

## 2 Theory

### 2.1 Real-Axis SLM Modulation

The SLM used in this paper is an AFLC SLM. The device was constructed by Boulder Nonlinear Systems. It has $128 \times 128$ pixels and a frame rate of 102 $\mu$s. The device is capable of modulating along the real axis, in an analog and a bipolar (i.e., positive and negative) manner.

The SLM pixels are approximately equivalent to quarter-wave plates with an electronically controllable optical axis. Since the device is reflective, it is operated in double pass, so it effectively acts like a half-wave plate. The SLM is placed behind a polarizing beamsplitter. The input polarization state is linear and aligned to bisect the maximum angles of the optical axes achievable by the SLM. If the optical axis of the SLM pixel is at an angle $\theta$ to the plane of polarization of the incident light, the reflected light will have been rotated by an angle $2\theta$. The polarizing beamsplitter is then used to select the polarization component orthogonal to the incident polarization, hence giving amplitude modulation. If the optical axis of the pixel is rotated $-\theta$, the outgoing light will be rotated in the opposite direction, leading an opposite amplitude modulation. This allows analog modulation along the real axis in both positive and negative directions.

### 2.2 Complex Modulation Technique

Complex modulation can then be achieved using a phase-detour technique. Combined phase and amplitude modulation can be represented using only two pixels, since the

pixel value can go negative. This is an improvement on the technique described in Ref. 12, which requires four pixels and, since they are all positive, results in a large dc bias. Our technique has been previously demonstrated by producing computer-generated holograms.[14]

The complex function to be encoded on the SLM, $F(x,y)$, is represented by an $N \times N$ array and is split into its real and imaginary parts. A $2N \times 2N$ array is produced, and the real data are written to every $2n$'th element in the $x$ direction, whilst the imaginary data are written to every $2n+1$'th element ($n=0,1,2,3,\dots$). Every second pair is negated to maintain a continuous $\pi/2$ phase lag over the four pixels.

If each SLM pixel is square and of width $b$, the complex function $f(x,y)$ can be represented by

$$
f_s = \mathrm{comb}\!\left(\frac{y}{b}\right) \sum_{n=-\infty}^{\infty} \delta(x-na)\, \exp(i\pi n)\, \mathrm{Re}f(x,y)
$$

$$
+ \mathrm{comb}\!\left(\frac{y}{b}\right) \sum_{n=-\infty}^{\infty} \delta\!\left(x-a\!\left(n+\frac{1}{2}\right)\right)
$$

$$
\times \exp(i\pi n)\, \mathrm{Im}f\!\left(x-\frac{a}{2},y\right), \tag{1}
$$

where Re means the real part, Im the imaginary part, and $a=2b$. This Fourier transforms to become

$$
F_s(\omega,\nu) = \frac{1}{2} \sum_{m=-\infty}^{\infty} \sum_{n=-\infty}^{\infty} F\!\left(\omega-\frac{n}{2a},\nu-\frac{m}{b}\right)
$$

$$
\times [1+\exp(-i\pi a\omega)][1-\exp(i\pi n)]
$$

$$
+ \frac{1}{2} \sum_{m=-\infty}^{\infty} \sum_{n=-\infty}^{\infty} F^*\!\left(-\omega-\frac{n}{2a},-\nu-\frac{m}{b}\right)
$$

$$
\times [1-\exp(-i\pi a\omega)][1-\exp(i\pi n)]. \tag{2}
$$

The function $F_s(\omega,\nu)$ only exists when $n$ is odd. The modulation factor $1\pm\exp(-i\pi a\omega)$ causes the normal and conjugate terms to be alternately blanked when the device is used as a computer-generated hologram. In the hybrid correlator system the function $F(\omega,\nu)$ is the result of the FFT of the input signal mixed with the filter. In the hybrid method the result is the intensity pattern from Eq. (2), $F_s(\omega,\nu)F_s^*(\omega,\nu)$, where in this case $f(x,y)$ is the FFT of the input scene to the correlator multiplied by the filter.

In the optical correlator system only the filter is placed on the SLM, so just after the filter the signal is represented by

$$H_s(\omega,v)G(\omega,v)$$

$$= \frac{1}{2}\left[\text{comb}\left(\frac{\omega}{2a},\frac{v}{b}\right)\right.$$

$$\left. -\text{comb}\left(\frac{\omega-a}{2a},\frac{v}{b}\right)\right]H(\omega,v)G(\omega,v)$$

$$+\frac{1}{2}\left[\text{comb}\left(\frac{\omega}{2a},\frac{v}{b}\right)-\text{comb}\left(\frac{x-a}{2a},\frac{v}{b}\right)\right]$$

$$\times H^*(\omega,v)G(\omega,v)+\frac{1}{2}\left[\text{comb}\left(\frac{\omega-a/2}{2a},\frac{v}{b}\right)\right.$$

$$\left. -\text{comb}\left(\frac{\omega+a/2}{2a},\frac{v}{b}\right)\right]H\left(\omega-\frac{a}{2},v\right)G(\omega,v)$$

$$-\frac{1}{2}\left[\text{comb}\left(\frac{\omega-a/2}{2a},\frac{v}{b}\right)-\text{comb}\left(\frac{\omega+a/2}{2a},\frac{v}{b}\right)\right]$$

$$\times H^*\left(\omega-\frac{a}{2},v\right)G(\omega,v), \tag{3}$$



**Fig. 2** A simulation of the hybrid and 4-f correlator results. The graph shows the peak intensity of the correlation as the input signal is moved across the field. Solid curve: hybrid; dashed curve, 4-f.

where $g(x,y)$ is the input signal, $G(\omega,v)$ is its Fourier transform, $H(\omega,v)$ is the Fourier space filter function, and $h(x,y)$ is its Fourier transform. The output field is represented by the Fourier transform of Eq. (3):

$$h(x,y)\otimes g(x,y)$$

$$=\frac{1}{2}\sum_{m=-\infty}^{\infty}\sum_{n=-\infty}^{\infty}h\left(x-\frac{n}{2a},y-\frac{m}{b}\right)$$

$$\times[1+\exp(-i\pi ax)][1-\exp(i\pi n)]\otimes g(x,y)$$

$$+\frac{1}{2}\sum_{m=-\infty}^{\infty}\sum_{n=-\infty}^{\infty}h^*\left(-x-\frac{n}{2a},-y-\frac{m}{b}\right)$$

$$\times[1-\exp(-i\pi ax)][1-\exp(i\pi n)]\otimes g(x,y). \tag{4}$$

Again the factor $1\pm\exp(-i\pi ax)$ causes the conjugate and normal terms to be alternately blanked so that a series of correlation spots are created off axis.

### 2.3 Effect of Modulation Term

The modulation term causes the filter function $f(x,y)$ to be modified from the ideal. The amplitude of the function drops off as $|x|$ increases. There is also a phase wedge introduced across $f(x,y)$. Computer simulations of this effect were performed to assess it. Figure 2 (dashed line) shows a computer simulation of an all-optical correlator using the complex filter. A spot was moved across the input field and correlated with a single spot. The maximum intensity of the resulting correlation is shown. A correlation peak was produced as expected. However, it was shifted off axis. The simulation was also performed for the hybrid correlator. The normalized peak intensity as the spot is moved is shown in Fig. 2 (solid line). In the conventional all-optical correlator there is no intensity variation across the output field as the spots are shifted. For the hybrid correlator, however, there is a clear dropoff in performance off axis.
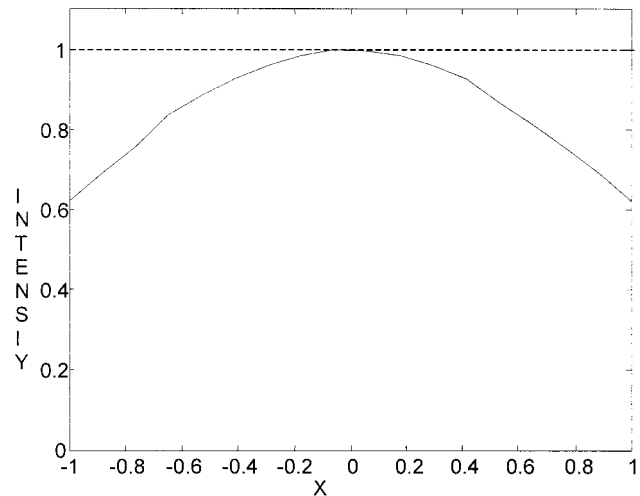
The lack of intensity dropoff in the conventional correlator system is because the reference object used to generate the actual filter is on axis and it is $g(x,y)$ that contains the shift. Since $g(x,y)$ is optically Fourier-transformed, it is not affected by any shortcomings of the complex data encoding on the SLM.

In the hybrid correlator the intensity dropoff as $|x|$ increases comes from the intensity modulation factor in Eq. (2). In addition to this, a conjugate factor will also start to appear as the spot is moved off axis. This does not effect the hybrid correlator when real-only or binary-phase-only filters are used. An example simulation of the hybrid correlator is shown in Fig. 3. In this case an on-axis letter A is correlated with itself. Two large peaks are visible. These are the terms generated when $n=\pm 1$ in Eq. (2). These two terms are the correlation peaks produced by the first positive and first negative diffraction orders.
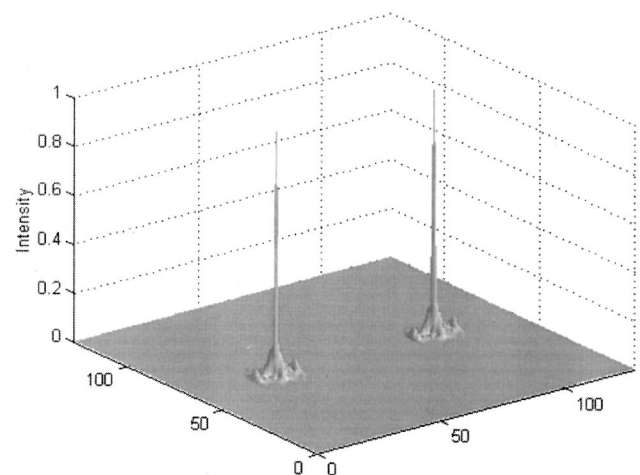


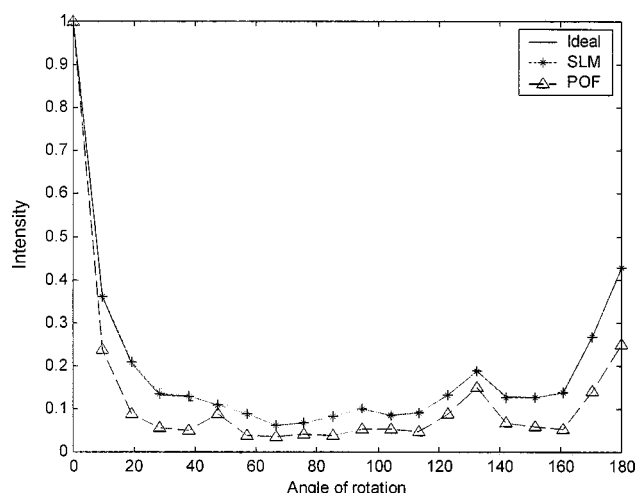**Fig. 3** Simulation result for the hybrid correlator.

**Fig. 4** Simulation result comparing an ideal matched filter, the SLM filter, and the phase-only filter (POF). The *x* axis represents the rotation angle of the input. The *y* axis is the correlation peak intensity (COPI).



**Fig. 5** The results of the optical correlator with a complex filter.

### 2.4 *Comparison with Ideal Filter*

Computer simulations comparing the phase-detour encoding of a complex filter with an ideal matched complex filter that could represent complex data with a single pixel were carried out. Figure 4 shows the normalized maximum intensity of the correlation of a letter A that is rotated through 180 deg. A phase only filter simulation is also shown for comparison. The response of the phase-detour filter is identical to that of the ideal filter graph. As expected, the phase-only filter is more intolerant of object rotation.

### 3 Experimental

The filter was set up in an all-optical correlator. The input filter was a photographic negative, and the light source was a 514.5-nm Ar ion laser. The SLM is controlled using a IBM-compatible PC. Data are written into an 8-bit frame store located on the SLM's driver board. This is done over the ISA bus on the PC. The frame store holds a total of 16 images, and these can be written to the actual SLM with a maximum frame rate of 102 $\mu$s, although a second negative frame is required to maintain a zero dc electric field across the liquid crystal.

Figure 5 shows an example result of the all-optical correlator. The input signal is shown in Fig. 6; the filter selects one of the A's. The correlation peak is quite large, since an 800-mm-focal-length lens was used. It is also located off axis. Figure 7 shows the same setup, but the imaginary data have been blocked. Since it now a real-only filter, the correlator cannot differentiate between the two A's.

Figure 8 shows an example result with the same input and filter function except using the hybrid correlator. The correlation spot is smaller in this case, since a faster lens can be used because there is no longer need to match the spectrum of the input signal to the filter.

### 4 Discussion

The optical correlator produces a correlation peak off axis that comes from the factor $-1/2a$ in Eq. (4). The hybrid system a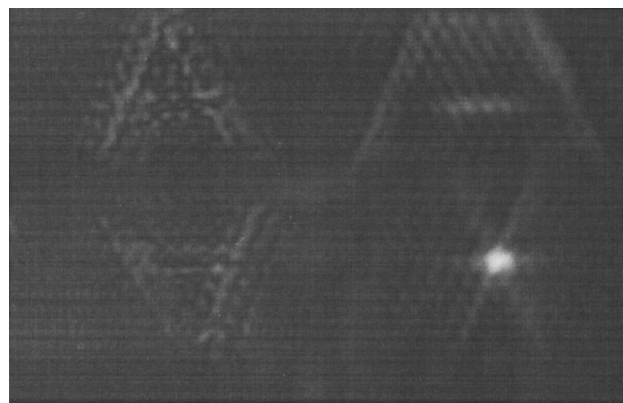lso produces a correlation peak off axis. In this case, the peak appears a quarter of the way from the zeroth order to the first order produced by diffraction from the SLM pixelation.

The hybrid system was considerably easier to set up than the optical system, since only one optical Fourier transform is required. However, it has worse off-axis performance than the all-optical correlator. This is caused by the appearance of a conjugate image in the output field and a reduction in intensity of the correlation peak. The reduction in intensity was limited to 60% in computer simulations and may not be a problem for some applications. Despite this limitation, the hybrid method still has many of the advantages over the all-optical method, such as robustness and compactness, as described above.
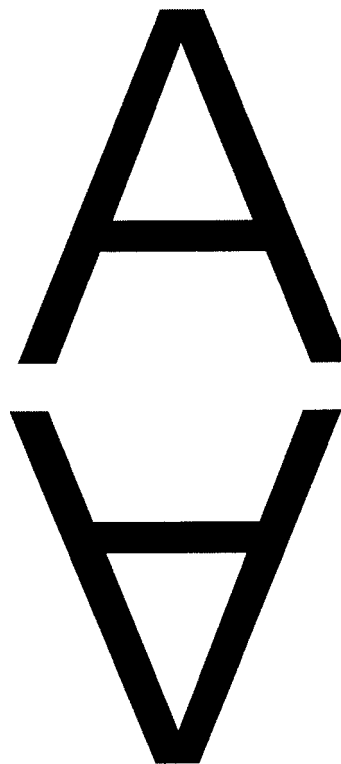


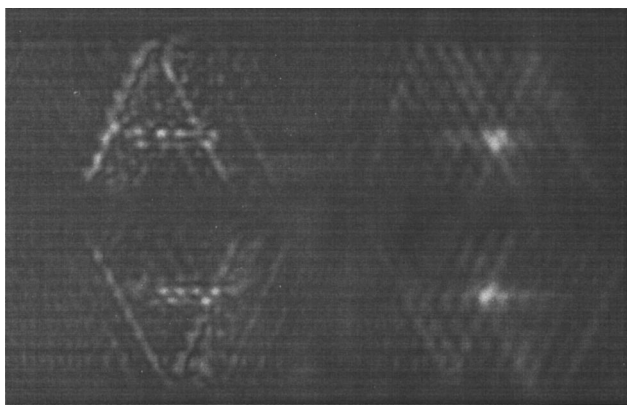**Fig. 6** The input mask for the optical correlator.

**Fig. 7** The optical correlator with a real-only filter.

### 4.1 Pixel Shape

The SLM pixels are all square so if the data are arranged into a $2 \times 1$ macro pixel, there will be a rectangular output field. For the all-optical correlator this was overcome by doubling the macro pixels up, making a $2 \times 2$ square. Equally valid methods to overcome this problem could be to have rectangular pixels or modify the filter design so that there was a nonsymmetric sampling rate in both directions. In the case of the hybrid correlator, the pixels could simply be left with a $2 \times 1$ ratio, which would give a rectangular output field.

### 4.2 Computational Overheads

In the hybrid system there are computational overheads to be considered when choosing which filters to implement. The overheads for the FFT system have previously been discussed in Ref. 4 and experimentally demonstrated to perform a $512 \times 512$ FFT in under 40 ms. For the filter, the simplest case is a BPOF. For a $128 \times 128$ SLM, 16,384 exclusive-or (XOR) operations are required, increasing to 262, 144 for a $512 \times 512$ device. The XOR is a relatively simple binary operation and can be performed using the two SHARC chips dedicated to the process. Each XOR operation takes 3 cycles of the 40-MHz processors, so it can be achieved in $10 \mu s$. The same number of operations are required for analog phase and real-only filters, except in
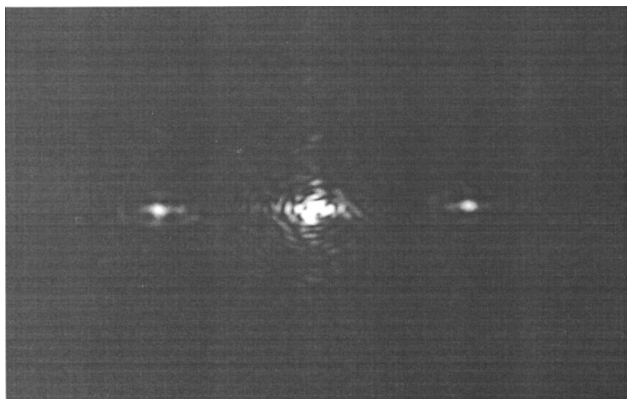
this case the operators are additions and floating-point multiplications, respectively, which are computationally more expensive and take 300 $\mu$s in the $128 \times 128$-pixel case. The filters will require the same number of addition operators plus a remainder operation to find the phase over the range 0 to $2\pi$ or the amplitude over $-1$ to 1. A lookup table or polynomial multiplication will then also have to be performed to get the correct drive voltage for the SLM pixel. The computationally most challenging filter type is the complex filter, which will require four multiplication and two additions per datum. However, the number of pixels has been halved in one dimension, so only about 1 ms is required.

## 5 Conclusions

A complex filter design has been demonstrated using an AFLC SLM. The filter requires two pixels grouped together and uses a phase-detour technique. An all-optical correlation demonstration has been shown, along with results from a hybrid correlator. The hybrid correlator provides a simpler and more robust solution to implementing a traditional 4-f optical correlator design.

*References*

1. A. B. Vander Lugt, "Signal detection by complex spatial filtering," *IEEE Trans. Inf. Theory* **10**, 139–145 (1964).
2. D. Psaltis, E. G. Paek, and S. S. Venkatesh, "Optical image correlation with a binary spatial light modulator," *Opt. Eng.* **23**(6), 698–704 (1984).
3. D. Carrott, G. Mallaley, R. Dydyk, and S. Mills, "Third generation miniature ruggedized optical correlator (MROC™) module," *Proc. SPIE* **3386**, 38–44 (1998).
4. R. Young, S. Huang, G. Li, T. Koukoulas, M. Heywood, D. Budgett, and C. Chatwin, "Implementation and performance considerations of hybrid digital/optical correlator configurations," *Proc. SPIE* **3715**, 16–31 (1999).
5. K. Bauchert, S. Serati, G. Sharp, and D. McKnight, "Complex phase/amplitude spatial light modulator advances and its use in a multi-spectral optical correlator," *Proc. SPIE* **3073**, 170–177 (1997).
6. T.-H. Chao, G. Reyes, and Y. Park, "Greyscale optical correlator," *Proc. SPIE* **3386**, 60–64 (1998).
7. C. Chatwin and R. Young, "Hybrid digital/optical correlator systems," presented at British Machine Vision Society Colloquium, Glasgow, 1993.
8. R. D. Juday and J. M. Florence, *Proc. SPIE* **3715**, 112–119 (1999).
9. J. M. Florence and R. D. Juday, "Full complex spatial filtering with a phase mostly DMD," *Proc. SPIE* **1558**, 487–498 (1991).
10. D. Mendlovic, G. Shabtay, U. Levi, Z. Zalevsky, and E. Marom, "Encoding technique for design of zero-order (on-axis) Fraunhofer computer-generated holograms," *Appl. Opt.* **36**, 8427–8434 (1997).
11. S. Serati and K. Bauchert, "Sampling technique for achieving full unit-circle coverage using real-axis spatial light modulator," *Proc. SPIE* **3715**, 112–119 (1999).
12. W. H. Lee, "Sampled Fourier transform hologram generated by a computer," *Appl. Opt.* **9**(3), 639–643 (1970).
13. C. B. Burckhardt, "A simplification of Lee's method of generating holograms by computer," *Appl. Opt.* **9**, 1949–1951 (1970).
14. P. M. Birch, R. C. D. Young, D. M. Budgett, and C. R. Chatwin, "Full complex optical modulation with an analogue ferroelectric liquid crystal spatial light modulator," *Opt. Commun.* **175**(4–6), 347–352 (2000).

**Fig. 8** The hybrid-correlator result. Two correlation peaks are visible on each side of the dc term.

**Philip Birch** obtained a BSc physics degree from the University of Durham, United Kingdom, in 1994 and then completed a PhD at the same institution in the field of liquid-crystal adaptive optics. Since 1997, he has been working as a research fellow at the University of Sussex, where his research interests include diffractive optics, computer-generated holograms, liquid-crystal spatial light modulators, correlators, image recognition, and rapid prototyping.

**Rupert Young** graduated from Glasgow University in 1984 with a degree in engineering. Until 1993 he was employed in the Laser and Optical Systems Engineering Research Centre at Glasgow, during which time he gained wide experience in optical systems engineering and image/signal-processing techniques. He was awarded a PhD degree in 1994 for research into optical pattern recognition. In April 1995 he was appointed a lecturer, and in October 1998 a senior lecturer, in the School of Engineering, University of Sussex. Here, he is continuing research into various aspects of optical pattern recognition, digital image processing, and electro-optics system design, and applying this to a wide range of problems of industrial relevance.

**Frédéric Claret-Tournier** obtained a degree in signal processing in 1996 from the Electrical Engineering School of Grenoble, France; he then graduated with an MSc in digital electronics at the University of Sussex at Brighton, United Kingdom in 1997. Since 1998, he has been working as a research fellow at the University of Sussex, particularly developing control software for microstereolithography and hybrid digital-optical correlators where architecture and organization of signal processors is implemented.
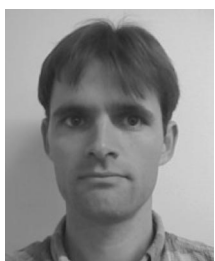
**David Budgett** graduated from Canterbury University, New Zealand, in 1989 with a first-class honors degree in electrical engineering. He pursued interests in medical technologies at Imperial College, from where he was awarded a PhD degree in 1995. He has developed novel systems for optical computing and high-speed pattern recognition at the University of Glasgow. During a two-year lecturing position at the University of Auckland, he developed multichannel data acquisition systems. In 1999 he took up a faculty position with the School of Engineering, University of Sussex. Here, he is continuing research into digital systems, image processing, rapid prototyping, and microrobotics.

**Christopher Chatwin** holds the Chair of Industrial Informatics and Manufacturing Systems (IIMS) at the University of Sussex, UK, where *inter alia*, he is director of the IIMS Research Centre and the Laser and Photonics Systems Research Group. Before moving to Sussex, he spent 15 years in the Engineering Faculty of the University of Glasgow, Scotland, where as a reader he was head of the Laser and Optical Systems Engineering Centre and the Industrial Informatics Research Group; during this period he ran a succession of major national and international interdisciplinary research programs. Prior to this he worked in the automotive industry. He has published two research-level books—one on numerical methods, the other on hybrid optical digital computing—and more than 100 papers, which focus on optics, optical computing, signal processing, optical filtering, holography, laser materials processing, laser systems and power supply design, laser-physics beam-target interactions, heat transfer, knowledge-based control systems, expert systems, computer integrated manufacture, CIM scheduling, manufacturing communication systems, computational numerical methods, genetic algorithms, maximum-entropy algorithms, chaos, robotics, instrumentation, digital image processing, intelligent digital control systems, and digital electronics. Professor Chatwin is on the editorial board of the international journal *Lasers in Engineering* and is editor of the RSP/Wiley book series on Industrial Informatics and Integrated Manufacturing Business Systems. He is a member of the Institute of Electrical and Electronic Engineers, SPIE, the European Optical Society, the Association of Industrial Laser Users, and the Laser Institute of America; a senior member of the Society of Manufacturing Engineers; and a member of the New York Academy of Sciences. He is a Chartered Engineer, a Euro-Engineer, a Chartered Physicist, and a Fellow of the Institute of Electrical Engineers, the Institute of Mechanical Engineers, and the Institute of Physics.